Polarization Behavior of Vertical-Cavity Surface-Emitting Lasers: Experiments, Models and Applications

Krassimir Panajotov*, Jan Danckaert, Guy Verschaffelt, Michael Peeters, Bob Nagler, Jan Albert, Boris Ryvkin**, Hugo Thienpont, and Irina Veretennicoff

Vrije Universiteit Brussel, Department of Applied Physics & Photonics,
Pleinlaan 2, B-1050 Brussels, Belgium
Tel. +32 2 629 3658 Fax +32 2 629 3450
e-mails: kpanajotov@alna.vub.ac.be; kpan@issp.bas.bg
**Permanent address: Institute of Solid State Physics, 72 Tzarigradsko Chaussee blvd., 1784 Sofia, Bulgaria*
***Permanent address: A.F. Ioffe Physicotechnical Institute, 194021 St. Peterburg, Russia*

Abstract. Due to the emission of light perpendicular to the surface of the quantum well and the usually symmetric vertical resonator there is a priori no intrinsic polarization anisotropy mechanism in VCSELs. Small residual strain explains the emission of linearly polarized light with a common orientation along [110] or [1-10] crystallographic directions. These two modes of linear polarization are strongly anti-correlated. Experimentally, polarization switching between them can be observed with increasing the injection current. It could happen from shorter to longer wavelength mode (type I) or in the opposite way – from longer to shorter wavelength mode (type II). The polarization switching happens through a region of mode hopping or hysteresis. In the first case, the dwell time (the average time the laser spends in one mode) scales in several orders of magnitude. Thermal (carrier) effects influence the polarization behavior of VCSELs through the red (blue) shift of the gain maximum and through the dependence of the losses on the photon energy and temperature. Also, internal or external stress strongly affects the polarization behavior of VCSELs, giving rise to refractive index and gain anisotropy. In principle, one has to consider different gain curves for different orientation of the light polarization. Such two - gain - curve gain equalization model could explain type I polarization switching followed by type II polarization switching. In order an abrupt switch to exist, gain nonlinearities have to be taken into account. It is possible that the spin-flip dynamics is playing an essential role during the polarization switch. Finally, we show one straightforward implementation of polarization switching in VCSELs, e.g. reconfigurable interconnects.

I. INTRODUCTION

Semiconductor lasers with vertical cavity and emission perpendicular to the surface of the active layer were suggested by Iga et al in 1979[1]. Pulsed and CW room temperature operation were achieved in 1984[2] and 1988[3], correspondingly. In the beginning of Nineties, the advance in VCSEL design and growth was tremendous,

CP560, *Nanoscale Linear and Nonlinear Optics,* edited by M. Bertolotti, et al.

resulting in devices comparable with and even surpassing the conventional edge emitting lasers (EEL) in threshold currents, efficiencies and speed of modulation. Nowadays, many laboratories and companies develop VCSEL technologies because of their inherent advantages. In the EEL the optical modes are determined by the transversely very thin and laterally wide heterostructure gain region. This results in a highly elongated, quite divergent optical beam. The long (hundreds of μm) optical cavity supports multiple longitudinal modes resulting in lasing on several modes or mode hopping. As a result EELs are always working at the gain peak. Because the active medium is placed all-along the cavity, it provides sufficient gain and the reflectivity of the cleaved laser surfaces is enough for achieving lasing. But optical testing can only be performed after cleaving or etching. In VCSELs, the gain/index-confining aperture transversely determines the optical modes. It is easily made circular to facilitate the coupling to optical fiber. The beam divergence is drastically reduced (to about 10 degrees). The very short cavity length supports a single longitudinal mode. Surface emission makes possible two-dimensional arrays to be fabricated with high fill factor. Additionally, the fabrication process can make use of the standard technologies for integrated circuits and on wafer testing is possible. All these advantages of VCSELs could only be realized after overcoming significant technology difficulties. As the gain region (multiple quantum wells) occupies a tiny part of the cavity, a high-quality cavity is necessary to compensate for the significant reduction of the single-pass gain in comparison with the ELLs. Distributed Bragg reflectors (DBR) with 20 to 40 pairs are grown to achieve a reflection coefficient in excess of 99%. As the current has to flow through the DBR, delta doping and alloy grading of the hetero-interfaces in the p-type DBR are used to reduce the electrical resistance.

The simplest method to achieve optical and carrier lateral confinement is to etch a pillar or a post. The first monolithic VCSEL were air-post ones[4]. Reactive ion etching or chemically assisted ion beam etching make possible the fabrication of pillar structures with small cross-section areas and smooth vertical surfaces. Strong index guiding is present in air-post VCSELs because of the large refractive index difference between semiconductor and air. A planar VCSEL geometry provides better thermal dissipation and simplifies fabrication and packaging. Lateral carrier confinement is possible in planar structures by selectively implanting ions to damage and insulate certain regions of the upper DBR[5]. Small apertures are however difficult to define because of ion straggling. The ion - implanted VCSELs are gain guiding, that is, there is no optical confinement as the refractive index of the implanted region is the same as of the rest of the structure. Nevertheless, index guiding due to thermal effects is observed under CW operation, because the current flow heats up the central region of the laser and forms a thermal lens via thermo-optic effect[6]. Thermal lensing is identified from the higher threshold current for pulse current than for DC current. Typically the threshold current and threshold voltage are higher for proton-implanted VCSELs than for the air-post ones. Wet oxidation of AlGaAs was a major break-through in the VCSEL state of the art[7]. The oxide aperture provides very effective current and optical confinement and results in significant improvement of VCSEL performance. The oxidation starts at the exposed sides of the mesa and propagates towards the center of the Al-rich layer placed at the desired location for current and

optical aperture. This could be significantly closer to the gain region resulting in less carrier diffusion effects. The optical confinement, i.e. the effective index difference between the cavity region and the Al_xO_y region could be controlled through the thickness and the position of the oxide layer[8]. Oxide confined VCSELs now hold several performance records: the lowest threshold current (<10 μA) than any other laser diode[9], the lowest threshold voltage (1.33V at 970nm)[7], the highest power conversion efficiency (>50%)[10] and the highest small-signal modulation bandwidth (>20GHz)[11].

In this paper we will focus on the polarization properties of VCSELs with different structures but working mainly in a single mode regime. In section II, we present a variety of experimental results on polarization switching (PS) in VCSELs. In section III, we discuss the physics behind PS in VCSELs and present a number of different explanations. In section IV, we give some applications of PS in VCSELs, already demonstrated.

II. POLARIZATION SWITCHING IN VCSELS: EXPERIMENTAL RESULTS

The polarization properties of the light emitted by a semiconductor laser are determined by the polarization properties of the gain, i.e. by the interband optical transition matrix element, and by the polarization properties of the optical cavity. Because of VCSEL surface emission the transition matrix element is the same for all light polarization directions in the plane of the active layer. Moreover, the Conduction Band (CB) - Heavy Hole (HH) transitions are dominant (the band-edge value of the transition matrix element is 1/2 compared to 1/6 for CB - light hole (LH) transitions) implying that mainly CB-HH transitions determine the form of the gain. This is in clear contrast with what happens in EELs, where the transition matrix element is different for light polarized in the plane of the QW and perpendicular to it. Also, mainly CB-HH transitions contributed for the in-plane polarized emission while mainly CB-LH transitions contribute to the out-of-plane polarized emission. The optical confinement is also different in VCSELs and EELs: usually a symmetric cylindrical or rectangular aperture is defined by oxidation, air-post or proton-implantation in VCSELs. On the contrary, the different lateral and transverse dimensions of the EEL waveguide give rise to waveguiding and reflectivity anisotropy. In summary, *in contrast with EELs there is no intrinsic polarization anisotropy mechanism in VCSELs.*

Nevertheless, VCSELs do emit linearly polarized light along the [110] and [1-10] cristallographic directions[12]. This has been attributed to residual stress after manufacturing and/or to the electro-optic effect[13,14], leading to cavity in-plane birefringence[13,14]. As a result, two linearly polarized modes with slightly different wavelengths and consequently with slightly different gains are supported by the VCSEL cavity. Experimentally, it is found that these two modes do not lase simultaneously and that sometimes when the injection current is increased switching between them occurs[15-19]. A polarization resolved Light versus Current (LI) characteristic of proton-implanted GaAs/AlGaAs QW VCSEL emitting around 850 nm is shown in fig.1[17]. PS is observed in the fundamental Gaussian transverse mode when operating with direct current (DC) but not for short-pulse current operation. The current

at which the PS occurs changes from one laser to another. It also depends on the laser substrate temperature. Looking at the spectrum of the emitted light, we identify the PS to be from higher frequency ν_H mode (thin line) to lower frequency ν_L mode (thick line). We shall refer to such kind of PS as type I PS because it is the first one reported[7] and in order to distinguish from the opposite way of switching, namely from lower to higher frequency polarization mode which we call type II PS.

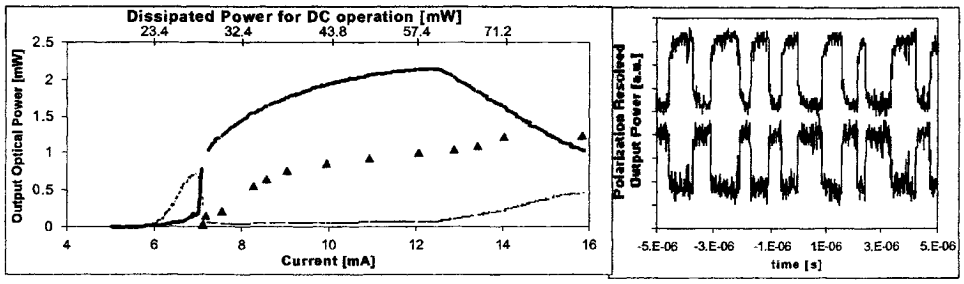

FIGURE 1. (left) LI curve showing PS for DC current (ν_H (ν_L) mode as thin (thick) line) but not for short-pulse current (triangles). (right) Time trace of the polarization resolved optical output in the region of PS showing mode hopping behavior.

Although we see an abrupt PS in the steady-state LI curve, we observe that the laser continuously jumps between the two well-defined states if the VCSEL is biased in the PS region (fig.1 - right). The time traces of the two polarization modes as observed with fast detectors are shifted vertically for clarity. One can see the perfect anti-correlation between the two polarization resolved intensities[17]. The time that the laser stays in one mode changes randomly with a mean value called *dwell time*. If the current where the polarization switching occurs is changed, the dwell time changes in the range of several order of magnitudes. Experimentally, we have observed scaling of the dwell time with current of PS from tens of nanoseconds to seconds (fig.2)[20].

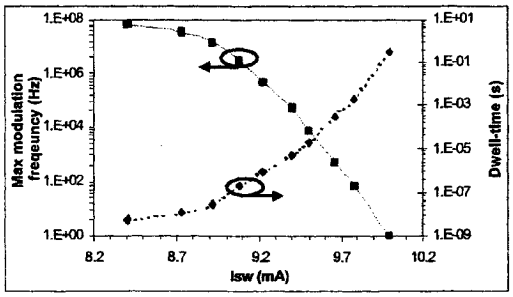

FIGURE 2. Scaling of the dwell time and maximum modulation frequency with the current of PS.

We bias the VCSEL in the region of mode hopping and modulate it with a small electrical signal, PS by current modulation is obtained (fig.3). For a frequency of 30 MHz perfect PS is observed (fig.3 left), while at 50 MHz the laser starts to miss the polarization switch from time to time being only intensity modulated at these events (fig.3 right)[21]. In such a way, one can define a maximum small signal modulation frequency for PS which in this case is around 30 MHz. Together with the dwell time, which exponentially increases with the PS current[20], the maximum modulation frequency for a given amplitude of the modulation signal scales in a similar but reverse way (fig.2). This behavior is quite similar to the mode hopping between two

longitudinal modes in edge emitting lasers[22]. This similarity suggests that the polarization mode-hopping is related to spontaneous emission noise driven dynamics of a VCSEL working in two longitudinal mode regime rather than to the fact that these two modes have orthogonal polarization.

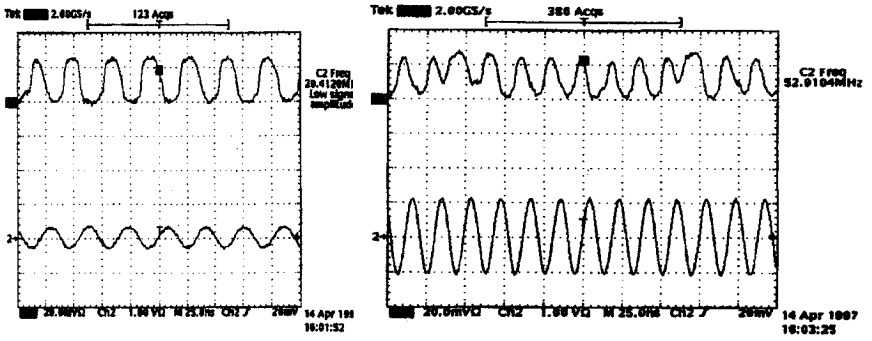

FIGURE 3. Small signal modulation around PS current: the modulation signal is the bottom trace and the polarization resolved optical signal is the top trace.

A typical feature for VCSELs is that the LI curve is not linear: the slope of the LI curve saturates with current as seen in fig.1. Moreover, if the current is further increased the slope of the LI curve becomes negative and the lasing action ceases. This behavior is due to the current self-heating of the laser combined with the single longitudinal mode operation. As the gain curve redshifts much faster with temperature than the cavity mode, the eventual misalignment between the gain maximum wavelength and the cavity wavelength prevents lasing.

The kink in the LI curve, that is clearly visible in fig.1, appears for currents that depend on the size of the VCSEL aperture. It is a signature for the appearance of a next order transversal mode, in this case the LP_{11} mode. This is mainly due to spatial hole burning effect which will be discussed in the next section.

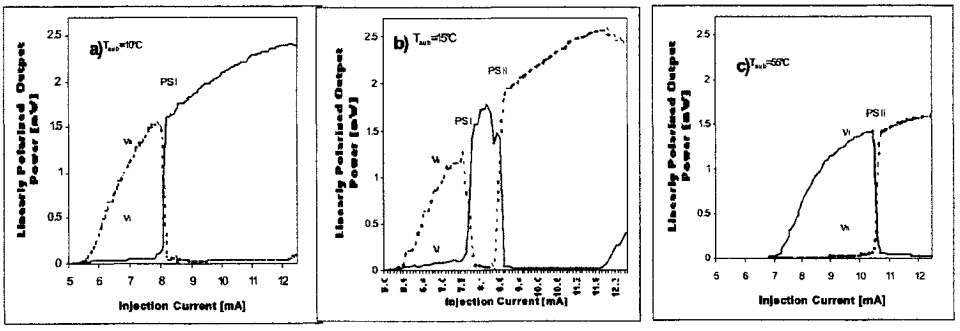

FIGURE 4. Polarization resolved optical output power versus DC injection current characteristic at different substrate temperature: a) T_{sub}=10°C, b)T_{sub}=15°C and c) T_{sub}=55°C. Lower (higher) energy mode is shown as full (dashed) line.

We have also studied how the laser substrate temperature influences the polarization behavior of VCSELs[23]. Fig.4 shows three typical LI curves for DC operation at fixed substrate temperatures of 10°C, 15 °C and 55°C. It is seen that at low substrate temperature (10°C) only type I PS takes place (fig.4a). At T_{sub}=15C (fig.4b) two types of PS occur: from ν_H mode to ν_L mode (type I PS) followed by a second one in the opposite direction (type II PS). At higher substrate temperatures T_{sub}=25°C – 55°C only type II PS takes place (fig.4c T_{sub}=55°C). The frequency splitting between the two modes of orthogonal linear polarization is 12 GHz and remains constant in the range of substrate temperatures for which these measurements are taken.

Although one could expect the PS to be influenced by the thermal waveguiding effect in the proton implanted VCSELs investigated above, we observe quite similar PS behavior for index-guiding VCSELs, namely the air-post VCSELs fabricated at CSEM, Zurich[24]. The lasers have three 8nm thick GaInAs quantum wells and GaAs/AlAs mirrors. They emit light around 980nm and show a threshold current of about 2.5mA. The polarization resolved LI curves and the optical spectrum are shown in fig.5. Again, PS of type I happens through a region of mode hopping. Similar scaling of the dwell time with current is observed[20,24].

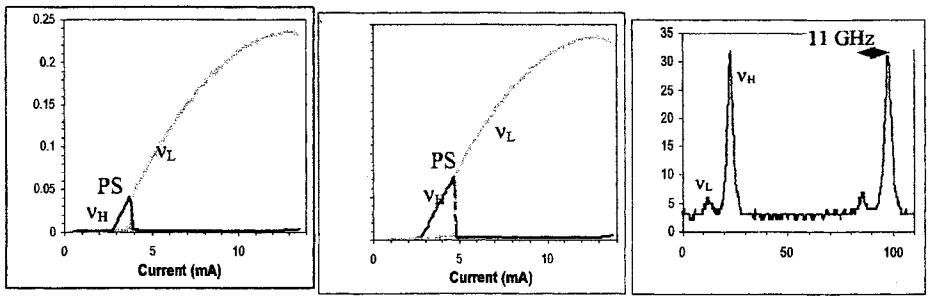

FIGURE 5. PS through mode hopping in air-post VCSELs. (right) The Fabry-Perot optical spectrum (left).

In oxide confined VCSELs quite different observations were made[24]. We investigated GaInAs quantum well VCSELs emitting around 960nm. When the oxide-aperture is very small (diameter 3-4 μm) the VCSELs are single-transverse mode up to the thermal rollover point at about five times the threshold current. A polarization switch of type I is observed between the two fundamental modes along [110] and [1-10] directions. Now, PS happens through a large region of hysteresis (fig.6a). This hysteresis region is also believed to exist in the proton-implanted and the air-post VCSELs, but it appears to be masked by the mode hopping behavior. Actually, the spontaneous emission noise drives the VCSEL from one polarization state to the orthogonal one due to the presence of bistability. Another difference in these oxide-confined VCSELs is the strong tuning of the PS current with substrate temperature. When the oxide-aperture is larger, VCSELs of the same structure operate in multiple-transverse modes. In this case, the upward PS is in the region where the first higher order transverse mode is already lasing while the downward PS is in the region of the

fundamental mode (fig.6b). Still the polarization switch is of type I between the fundamental modes with orthogonal polarization.

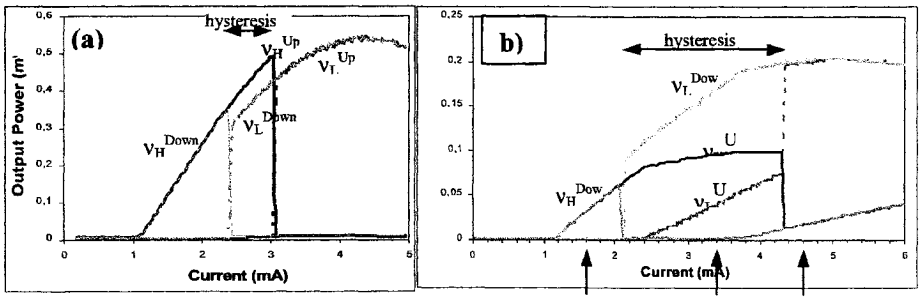

FIGURE 6. PS through hysteresis in oxide-confined VCSELs: (a) small aperture; (b) large aperture.

Last but not least, we investigated the impact of the anisotropic in-plane strain on the polarization characteristics of the lasers in all types of VCSEL structures. We introduced in-plane anisotropic strain in the VCSEL cavity via a homemade laser holder[25]. For uniaxial tensile strain along [1-10] direction of the laser wafer the laser is initially (at a small external stress) emitting in the low frequency mode (ν_L state). The direction of this linearly polarized state is at about 20° away from the [1-10] direction (fig.7a). Increasing the external stress, the direction of this polarization mode is continuously tuned towards the line of the tensile strain and remains in this orientation.

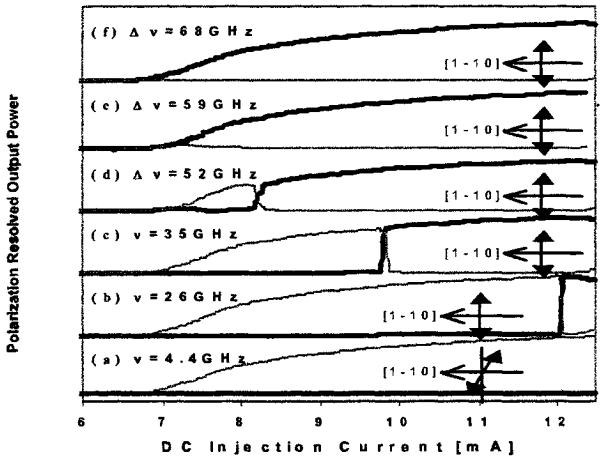

FIGURE 7.
Polarization resolved optical output power versus DC injection current for increasing tensile strain along [1-10] (A) and [110] (B) crystallographic direction. The higher (lower) frequency mode is shown by thick (thin) solid line. The orientation of the higher frequency linearly polarized mode is schematically shown.

Increasing the external stress the frequency splitting between the two linearly polarized modes also increases. PS in the fundamental mode is first observed when the strain induced frequency splitting becomes rather large (about 25GHz in fig.7b) and appears at quite a high current. This is PS type II[25]. The PS current continuously decreases as the external stress is further increased (figs.7c-d). A very broad region of stress –

induced PS tuning exists (frequency splitting from 25GHz to 60GHz). At about 60GHz the PS point is moved to threshold (fig.7f) and for larger frequency splitting the laser is emitting in the higher frequency mode only, with linear polarization oriented perpendicular to [1-10] direction of the laser wafer.

The mode suppression ratio M, defined as the ratio of the power of the primary polarization mode and the orthogonal polarization mode, as a function of the frequency splitting between these two modes is shown in fig.8a for different injection currents. As can be seen from this figure, M changes with the splitting: initially it continuously decreases, reaches a minimum at the PS point and increases afterwards. As the current and the substrate temperature are fixed, this is a signature that *the effective gain difference between the two modes has a minimum at the point of PS.*

In fig.8b the triangles show the experimentally determined orientation of one of the two linearly polarized eigenstates as a function of the frequency splitting. The solid line represents the calculated orientation of the index ellipsoid with respect to the crystal co-ordinate system if the induced birefringence via elasto-optic effect is taken into account. The only input parameters are the residual frequency splitting of 2 GHz and the initial orientation of this linearly polarized eigenstate of 15 degrees. The external strain is a dummy variable for the theoretical curve with a maximum value of 0.04%.

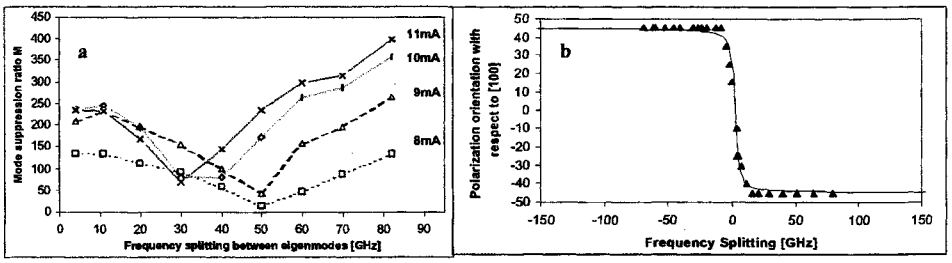

FIGURE 8. Mode suppression ratio (a) and polarization orientation in respect to [100] crystallographic direction (b) as a function of the frequency splitting induced by the in-plane anisotropic strain.

To summarize this section, we showed that VCSELs emit linearly polarized light (two fundamental modes with orthogonal directions). These two modes of linear polarization are strongly anti-correlated. PS (with injection current) is observed in all kinds of VCSELs: proton implanted, oxides confined and air post VCSELs. Different types of PS are identified: type I (ν_H->ν_L) and type II (ν_L->ν_H). PS can happen through a region of mode hopping or a hysteresis, in the first case the dwell time scales with current in eight orders of magnitude. Externally applied in-plane anisotropic strain strongly modifies the polarization behavior of VCSELs. In the next paragraph we will discuss a variety of physical phenomena which could explain these experimental results.

III. POLARIZATION SWITCHING IN VCSELS: DIFFERENT EXPLANATIONS

There is no consensus about the physics behind the PS in VCSELs. Different explanations have been suggested, which can be divided in two groups: the first one[26]

takes into account the finite spin-flip rate in semiconductor active material (SFM), and the second group takes into account the modification of the net gain with the current. This modification can be for the modal gain, determined by the overlap of optical field with the carrier distribution in the QW: thermal lensing[17] and spatial hole burning effects[27] contribute to such modification. The second sub-group of models considers the modification of the material gain and losses. This is due to the redshift of the gain maximum faster than that of the cavity modes[15]. The photon energy dependency of the losses is also considered[23] and QW in-plane anisotropy leads to two-gain curves[25].

SFM[26] considers the spin dynamics by dividing the carrier reservoirs (conduction band and HH valence band) into two two-level subsystems of different spin orientation (fig.9). Optical transitions are only allowed in each one of these two subsystems giving rise to left (E_-) and right (E_+) circularly polarized light. If an excess of carriers is created in one of the two subsystems, their spin flips to the opposite orientation with a rate γ_s. In addition, the phase - amplitude coupling, typical for the semiconductor lasers, is taken into account by the linewidth enhancement factor. VCSELs are described by four rate equations: two complex ones for the slowly varying optical field amplitudes, and two real ones for the total carrier density and the difference of the carrier densities in the two subsystems. The SFM model predicts that linearly polarized light should always be emitted of the VCSELs[26]. By taking into account the cavity anisotropy (birefringence and dichroism), PS is also predicted through a region of dynamical instabilities and/or hysteresis[28,29]. The SFM model can explain PS even for a very small dichroism and birefringence. It predicts reversible PS occurs from lower to higher frequency (type II PS). The SFM model could be simplified to only two equations, which allows for a phase space and bifurcation analysis[30]. The two types of switching can only be obtained if the SFM is combined with gain equalization model[31].

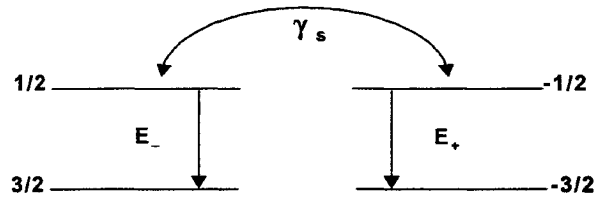

FIGURE 9. Schematic representation of the VCSEL carrier reservoirs (conduction band and HH valence band) divided into two two-level subsystems of different spin orientation.

The models focussing on the modification of the net gain with current can also explain PS in VCSELs. Indeed, the specific features of VCSELs: single longitudinal mode operation and current heating due to flow of the current through DBR-s lead to pronounced red-shift of the gain curve. This shift is faster than that one of the two cavity modes of different polarization. As a result, the laser will operate in higher frequency mode at the lower frequency side of the gain maximum and vice versa[15] (see fig.10 left), i.e. the higher frequency mode is selected when the gain derivative with respect to the photon energy is positive and vice versa. This model explains why type I PS takes place when transiting the gain maximum[15].

If one considers the photon energy dependence of the cavity losses this picture is modified[23]. Here the gain and loss derivatives with respect to the photon energy have to

be compared to determine which mode is lasing (see fig.10 right). The intervalence band absorption in the heavily p- doped DBRs decreases with increasing the photon energy, so that at the low photon energy side of the gain maximum the higher frequency (photon energy) mode is lasing. If the working point is at the high photon energy side of the gain maximum, either the lower or the higher frequency mode is lasing. Fast PS at constant lattice temperature can also be explained by carrier heating[32].

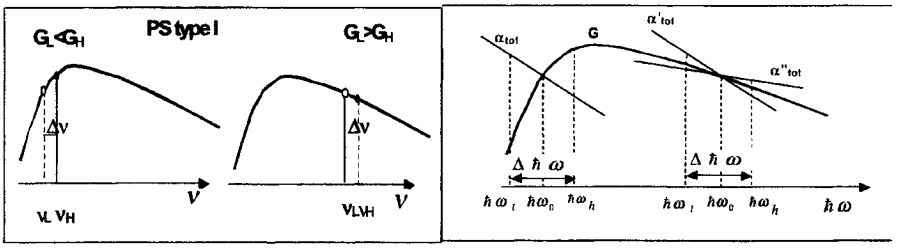

FIGURE 10. Schematic representation of the material gain and the two cavity modes: (left) gain curve redshift with current heating giving rise to PS type I; (right) the cavity losses are also shown as a function of photon energy.

However, the latter gain-shift related models can not explain our experimental results showing the strong dependence of PS on the external stress applied to the laser. To account for the effect of the anisotropic in-plane strain one should consider that it not only leads to birefringence via the elasto-optic effect but that it also results in a *different gain* for each of these modes. We can illustrate the effect of in-plane uniaxial strain by considering the Luttinger - Kohn Hamiltonian for the QW HH and LH bands and introduce the strain contribution according to the Bir-Pikus theory[33]. Valence band mixing takes place due to the existence of nondiagonal terms in the Hamiltonian[33].

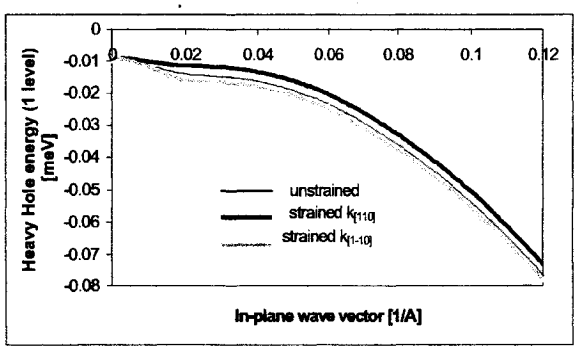

FIGURE 11. First HH QW level energy as a function of the in-plane crystal momentum along the [110] and [1-10] crystallographic directions.

In fig.11, the calculated energy of the first HH level as a function of the in-plane crystal momentum is shown. The thin solid curve represents the unstrained case for which the same dispersion curve is obtained along the [110] and [1-10] crystallographic directions. For the situation of tensile strain along [110] direction the dispersion of the HH energy along [110] and [1-10] crystallographic directions is different (respectively the thick black and the thick gray curves in fig.11).

Due to this anisotropy in the valence band energy dispersion relations, the gain will be different for different polarizations in the plane of the QW[34]. Because the maximum splitting is along the [110] and [1-10] crystallographic directions, the gain anisotropy will also be maximum along these two directions. Due to the strain-induced gain anisotropy, each linearly polarized state has its own gain curve on which it moves, as any relevant parameter (lattice and carrier temperature, carrier density, etc) is changed[25]. In addition to the strain-induced gain anisotropy, we have the gain difference due to the frequency splitting between the linearly polarized cavity modes which is also a result of the strain via the elasto-optic effect induced birefringence[25]. As the DC current is increased, the active region heats up and the gain will redshift faster than the cavity modes. Therefore, when working on the higher frequency side of the gain maximum, the carrier density should increase in order to keep the gain equal to the losses. To explain type II PS occurring on the higher frequency side of the gain maximum, two conditions should be met: 1) the linearly polarized mode with higher frequency has to show the larger gain (solid line in fig.12a) and 2) the two gain curves should move apart from each other with increasing current (fig.12b). In such a case the initial gain of the lower frequency mode is larger (fig.12a). But, when the two gains move apart as the current is increased, they become equal (fig.12b) and, eventually, the higher frequency mode will have the larger gain (fig.12c). It should be mentioned that in this picture, type II PS can be preceded by type I PS around the gain maximum. Such double PS has been experimentally demonstrated[23]. If instead of condition 1) the lower frequency mode has the larger gain, PS would not happen on the higher frequency side of the gain maximum. If, instead of condition 2), the two gain curves move closer to each other with increasing current, type I PS can still occur on the higher frequency side of the gain maximum[17].

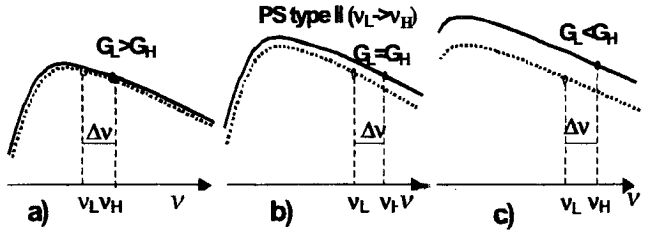

FIGURE 12. Scheme of the gain spectrum when a separate gain curve for each linearly polarized eigenstate is considered. Type II PS occurs on the higher frequency side of the gain maxima as the current is increased from (a) to (c).

In practice, one has to consider not only the material gain, but also the overlap of the optical field and the carrier density radial distributions, i.e. the modal gain. The modal gain can be changed due to change in the optical field pattern (by thermal lensing[17]) or the carrier distribution (by spatial hole burning[27]). Equalization of the modal gains for the two polarization modes with slightly different wavelengths can also occur in such a way.

We saw that a number of phenomena could lead to PS in VCSELs via equalization of the material or modal gains as the current and temperature are increased. This motivated us to consider the dynamics of PS in single-mode VCSELs in a phenomenological way. The two rate equations for the intensities of the two polarization modes are coupled by the third equation for the carrier density. Also the

gain compression is taken into account. If the two differential gains depend on the current (because of the current heating of the VCSEL), PS is obtained at the point of equalization of the gains as shown in the LI curve in fig.13 - left. Considering Langevin noise for the contribution of the spontaneous emission, one obtains mode hopping in the region of switching (fig.13 - right) and its scaling with the PS current. This simple model allows for analytical results for the time of PS and the dwell time[35].

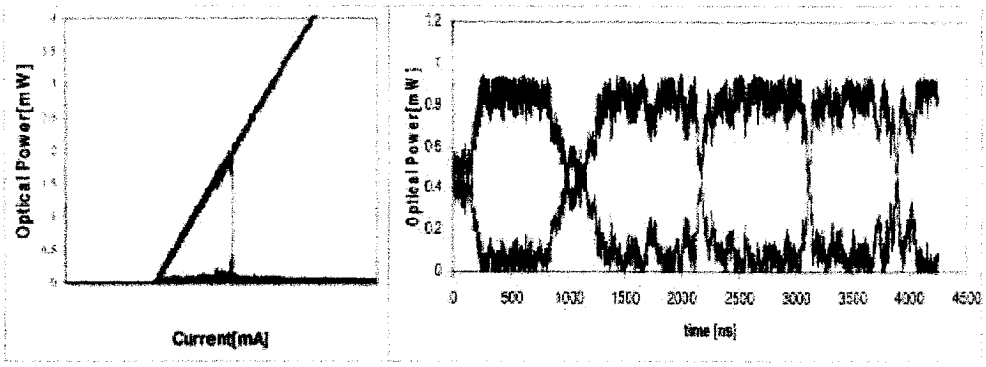

FIGURE 13. Simple intensity rate equation gain equalization model: (left) Polarization resolved LI curve showing PS at the point of gain equalization; (right) Mode hopping at the point of PS when Langevin noise term in included.

IV. POLARIZATION SWITCHING IN VCSELS: APPLICATIONS

The application of PS in VCSELs in sensing and data communication are only starting to emerge. Here we would like to report the work that was done on reconfigurable interconnects. The polarization of light gives an additional degree of freedom in information transport and routing. For example, the data stream is modulated in the intensity of the light and additional information can be added independently, by modulating its polarization direction[36,37]. This additional degree of

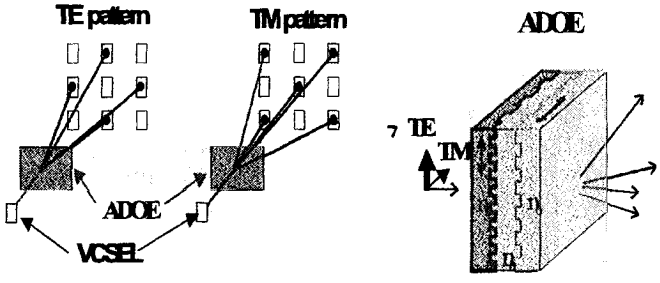

FIGURE 14. (left) Data transparent reconfigurable interconnects using polarization switching VCSEL and anisotropic diffractive optical element; (right) Anisotropic diffractive optical element (ADOE) consisting in two adjoined calcite plates with phase gratings etched in each of them.

freedom can be used for example, to change the interconnection pattern of free space optical interconnects. Different interconnection patterns are established for different polarizations of the light beam[36,37] (see fig.14 left). Such free-space reconfigurable

interconnects are playing an important role in digital parallel optical image processing. To demonstrate such a system we used anisotropic diffractive element (ADOE), i.e. optical device which diffracts the incident light of two orthogonal linear polarizations in two different arrays of spots and PS VCSEL (see fig.14 right).

The data are electrically superposed on top of a bias current(see fig.15 left), chosen such that it brings the VCSEL in one of its linear polarization eigenmodes (which we call TE and TM). In this way the VCSEL outputs data, which is routed by the ADOE in different directions depending on the value of the bias. If the bias is low the light is TE

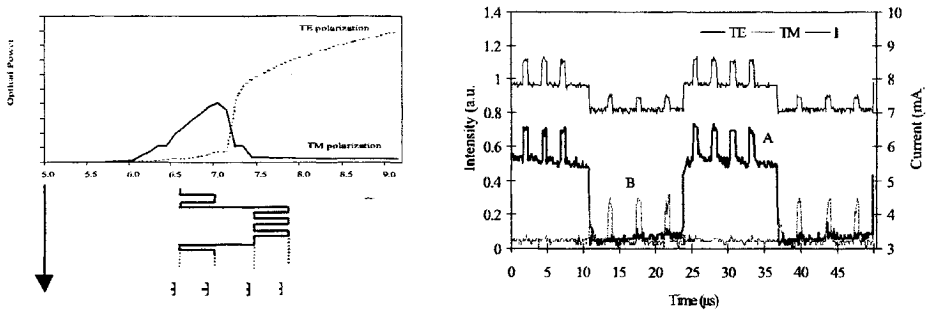

FIGURE 15. (left) LI curve and the way of modulation around PS current; (rght) Reconfigurable data transmission: traces A and B show the intensity in the TE and the TM generated spots (bottom) as a function of the voltage on the VCSEL (top).

polarized and the data signal is deflected in the horizontal direction onto detector A. In the case of a high bias the light is TM polarized and the data signal is deflected in the vertical direction onto detector B. The result is shown in the fig. 15(right). The upper trace shows the current through the VCSEL. The trace A (B) shows the intensity in one of the TE (TM) generated spots. A DC signal of different strength for the two linear polarizations is present in the detected data signal due to the different bias levels. With our equipment, we obtained a data bit rate of 1MHz and a reconfiguration rate of 40kHz[36]These modulation speeds were limited because of the maximum bit rate of the available function generator. In general, the reconfiguration speed is limited to 50MHz and the data bit rate can be several GHz. The speed limitation of 50 MHz of current induced PS in VCSELs can be overcome by using optical injection locking to induce the polarization switching[37]

From the view point of potential applications of polarization switching the frequency limitation of current induced polarization switching is a severe drawback. Moreover, this polarization switching is difficult to control and reproduce. Indeed, the two orthogonal polarization states correspond to two modes with frequencies that differ only by several GHz. As discussed, this frequency splitting is caused by a small birefringence due to elasto-optic and/or electrooptic effects that are difficult to control. In order to induce PS in a predictable and a controllable way, new VCSEL structures have been suggested and evaluated based on alternative mechanisms[38]. We propose two approaches to intracavity polarization modulation: one is relying on the electrooptical effect, in order to change the birefringence of the cavity, and the other relies on the electoabsorptive effect, in order to introduce anisotropic losses. Both approaches could

provide well controlled and fast switching between two orthogonal linearly polarized states[38].

V. CONCLUSSIONS

In this paper we discussed the polarization properties of VCSELs, especially the occurrence and characteristics of polarization switching. Due to the QW surface emission and the vertical resonator there is no a priori intrinsic polarization anisotropy mechanism in VCSELs. Small residual strain explains the emission of linearly polarized light, which is most commonly oriented along the [110] or [1-10] crystallographic direction. The two modes of linear polarization are strongly anti-correlated. Polarization switching with increasing the injection current occurs in all kinds of VCSELs: proton implanted, oxides confined and air post VCSELs. Different types of PS are identified: type I (ν_H->ν_L) and type II (ν_L->ν_H). PS can happen through a region of mode hopping or hysteresis, in the first case the dwell time scales over eight orders of magnitude with the PS current. Thermal (carrier) effects influence the polarization behavior of VCSELs through red (blue) shift of the gain maximum. Externally applied in-plane anisotropic strain strongly modifies the polarization behavior of VCSELs. Gain equalization models (gain+losses and/or two - gain model) can explain type I PS followed by type II PS. It is possible that the spin-flip dynamics is playing an essential role for PS. The application of PS in VCSELs in sensing and data communucation are only starting to be developed.

ACKNOWLEDGMENTS

The authors wish to acknowledge the Belgian Office for Scientific,Technical and Cultural affairs for the support in the framework of the Interuniversity Attraction Pole programme "Photonic Information Systems".JD, GV and BN acknowledge the FWO (Fund for Scientific Research - Flanders) for their fellowships and for purchase of laboratory equipment. This research also benefited from support by the Concerted Research Action "Photonics in Computing" and the Research Council (OZR) of the Vrije Universiteit Brussel.

REFERENCES

1. Soda, H., Iga, K., Kitahara, C., and Suemathsu, Y., *Jpn. J. Appl. Phys.* **18**, 2329-2330 (1979).
2. Iga, K., Ishikawa, S., Ohkouchi, C., and Nishimura, T., *Appl. Phys. Letters* **45**, 348-350 (1984).
3. Koyama, F., Kinoshita, S., and Iga, K., *Appl. Phys. Letters* **55**, 221-222 (1989).
4. Jewell, J. L., Sherer, A., McCall, S.L., Lee, Y. H., Walker, S., Harbison, J.P., and Florez, L.T., *Electron. Lett.* **25**, 1123-1124 (1989).
5. Tai, K., Fischer, R.J., Wang, K.W., Chu, S.N.G., and Cho, A.Y., *Electron. Lett.* **25**, 1644-1645 (1989).
6. Dutta, N.K., Tu, L.W., Hasnain, G., Zydzik, G., Wang, W.H., and Cho, A.Y., *Electron. Lett.* **27**, 208-210 (1991).
7. Choquette, K.D., Lear, K.L., Schneider, Jr., and Geib, K.M., *Electron. Lett.* **30**, 2043-2044 (1994).
8. Choquette, K.D., Schneider, Jr., Lear, K.L., and Geib, K.M., *Appl. Phys. Letters* **66**, 3413-3415 (1995).

9. MacDougal, M.H., Dapkus, P.D., Pudikov, V., Zhao, H., and Yang, G.M., *IEEE Phot.Techn.Lett.* **7**, 229-231 (1995).
10. Lear, K.L., Choquette, K.D., Schneider, Jr., Kylcoine, S.P., and Geib, K.M., *Electron. Lett.* **31**, 208-209 (1995).
11. Lear, K.L., Mar, A., Choquette, K.D., Kylcoine, S.P., Schneider, Jr., and Geib, K.M., *Electron. Lett.* **32**, 457-458 (1996).
12. Chang-Hasnain, C.J., Harbison, J.P., Hasnain, G., Von Lehmen, A.C., Florez, L.T. and Stoffel, N.G., *IEEE J. Quant. Electr.* **27**, 1402-1408 (1991).
13. Jansen van Doornen, A.K., van Exter, M.P., and J.P.Woerdman, *Appl. Phys. Lett.* **69**, 1041-1043 (1996).
14. van Exter, M.P., Jansen van Doorn, A.K. and Woerdman, J.P., *Phys. Rev. A.*, **56**, 845-583 (1997).
15. Choquette, K.D., Richie D.A., and Leibenguth, R.E., *Appl. Phys. Letters* **64**, 2062-2064 (1994).
16. Choquette, K.D.,.Lear, K.L, Leibenguth, R.E. and Asom, M.T., *Appl. Phys. Lett.* **64**, 2767-2769 (1994).
17. Panajotov, K., Ryvkin, B., Danckaert, J., Peeters, M., Thienpont, H., and Veretennicoff I., *IEEE Phot. Techn. Lett.* **10**, 6-8 (1998).
18. Martin-Regalado, J., Chilla, J.L.A., Rocca, J.J and Brusenbach, P., *Appl. Phys. Lett.* **70**, 3350-3352 (1997).
19. van Exter, M.P., Al-Remawi, A., and Woerdman, J.P, *Phys.Rev.Lett.* **80**, 4875-4878 (1998).
20. Verschaffelt, G., Albert, J., Peeters, M., Panajotov, K., Danckaert, J., Veretennicoff, I., Thienpont, H., Monti di Sopra, F., Eitel, S., Hoevel, R., Moser, M., Zappe, H.P., and Gulden, K., "Polarization switching and modulation dynamics in gain- and index-guided VCSELs" in *Vertical-Cavity surface-Emitting Lasers IV*, edited by Choquette, K. and Lei, C., Proceedings of SPIE 3946, SPIE, Washington, 2000, pp.246-256.
21. Panajotov, K., *Report for the Research Fellowship of the Belgium Ministry for Scientific, Technical and Cultural Affairs*, 1997.
22. Ohtsu, M., Teramachi, Y., Otsuka, Y., and Osaki, A., *IEEE J. Quant. Electr.* **22**, 535-543 (1986).
23. Ryvkin, B., Panajotov, K., Georgievski, A., Danckaert, J., Peeters, M., Verschaffelt, G., Thienpont, H., and Veretennicoff, I., *Journ. Opt. Soc. Am. B*, **16**, 2106-2113, (1999).
24. Verschaffelt, G., *Vertical-Cavity Surface-Emitting Lasers for parallel optical Datacommunication: polarization switching components and intra-MCM interconnects*, PhD Thesis, Vrijie Universiteit Brussels, Brussels, 2000.
25. Panajotov, K., Nagler, B., Verschaffelt, G., Georgievski, A., Thienpont, H., Danckaert, J., and Veretennicoff, I., *Appl. Phys. Letters* **77**, (2000).
26. San Miguel, M., Feng, O., and Moloney, J.M., *Phys.Rev.* **A52**, 1728-1739 (1996).
27. Valle, A., Pesquera L., and Shore, K.S., *IEEE Photon.Technol.Lett.* **9**, 557-559 (1997).
28. Martin-Regalado, J., San Miguel, M., Abraham, N.B., and Prati, F., *Opt.Lett.* **21**, 351-353 (1996).
29. Martin-Regalado, Balle, S., J., San Miguel, Valle, A., Pesquera, L., *Quantum Semiclass. Opt.* **9**, 713-736 (1997).
30. Erneux, T., Danckaert, J., Panajotov K., and Veretennicoff, I., *Phys.Rev.* **A59**, 4660-4667 (1999).
31. Balle, S., Tolkachova, E., San Miguel, M., Tredicce, J.R., Martin-Regalado J., and Gahl, A.,
32. B.Ryvkin and A. Georgievskii, *Semiconductors* **33**, 813-819 (1999).
33. Coldren, L.A., Corzine, S.W., *Diode Lasers and Photonic Integrated Circuits*, J.Willey & Sons, 1995, pp.488-536.
34. Burak, D., Moloney, J.V., and Binder, R., Phys.Rev. A, **61**, 053809, (2000).
35. Danckaert, J., Nagler, B., Albert, J., Panajotov, K., Veretennicoff, I., and Erneux, T., *IEEE J. Quant. Electr.* submitted.
36. Nieuborg, N., Panajotov, K., Goulet, A., Veretennicoff, I., and Thienpont, H., *IEEE Phot. Techn. Lett.*, **10**, 973-975 (1998).
37. Panajotov, K., Berghmans, F., Peeters, M., Verschaffelt, G., Danckaert, J., Veretennicoff, I., and Thienpont, H., *IEEE Phot. Techn. Lett.*, **11**, 985-987 (1999).
38. Ryvkin, B., Panajotov, K., Dackaert, J., Thienpont, H., Veretennicoff, I., "A New Type of Intracavity Electroabsorptive and Electrorefractive Polarization Modulation and Switching in VCSEL's", postdeadline paper in *Proceedings of Optics in Computing'98*, Bruge, Belgium, 17-20 June 1998.